Does a polymerized membrane crumple ?

A. Baumgärtner

Classification
Physics Abstracts
68.10C — 82.70K — 87.20C

Does a polymerized membrane crumple ?

A. Baumgärtner

Institut für Festkörperforschung, Forschungszentrum Jülich, D-5170 Jülich, Germany

(*Received 16 July 1991, accepted 29 July 1991*)

Abstract. — Evidence for crumpled conformations of polymerized membranes is reported. This is based on Monte Carlo simulations of flexible self-avoiding plaquette surfaces. The radius of gyration R scales with the surfaces area A according to $R^2 \sim A^{0.8}$. It is shown that the correlation function between plaquette normals $\langle \mathbf{n}(0) \cdot \mathbf{n}(x) \rangle$ decays rapidly to zero for plaquette membranes, in contrast to hard-sphere membranes exhibiting long ranged strong correlations. The probability distribution $P(\cos \theta)$ of enclosed angles between adjacent plaquettes is discussed with respect to differences between plaquette and hard-sphere membranes.

1. Introduction.

Polymerized (or tethered) membranes can be considered as two-dimensional analogs of linear polymers [1] and are realized, e.g., in cross-linked polymer sheets or in protein networks of biomembranes [2]. Similar as in the case of polymers, polymerized membranes are expected to collapse in poor solvent and to exhibit swollen conformations under good solvent conditions.

An important but still controversial question is concerned with the conformations of self-avoiding polymerized membranes under the local constraint of temperature dependent resistance against bending. At low temperatures the membrane is expected [3] to exhibit « flat conformations » with a fractal dimension $D = 2$ due to the resistance to in-plane shear deformations, which leads to an anomalous stiffening of the surface in the presence of thermal fluctuations. With increasing temperature the membrane is expected to undergo a transition to « crumpled conformations » [4, 5] which are self-similar and characterized by a fractal dimension $D = 2.5$.

However, the expected crumpled phase has never been observed in simulations of self-avoiding surfaces [6-12], but instead evidence has been given that self-avoiding tethered membranes are flat at all temperatures and relevant fluctuations are found only in the direction parallel to the average surface normal (« rough phase »). This is in disagreement with mean field estimates [5, 13] and recent experimental results [14].

It is important to point out, that our current evidence against a « crumpling phenomena » is based solely on simulations of a particular membrane model, the « pearl-membrane » consisting of tethered hard spheres. Since in this model the ratio between the diameter $\ell_{\min}$ of the hard sphere and the extended length $\ell_{\max}$ of the tether has to be chosen

approximately $\sigma \equiv \ell_{min}/\ell_{max} > 0.5$ in order to maintain the self-avoidance of the surface during the simulations of this model [5-12], we suspect that the spheres induce long range correlations between the triangles, which prevents the surface to crumple. In fact, it has been pointed out [12], that second neighbor repulsions only between spheres are sufficient to suppress crumpled conformations.

Therefore it seems obvious to look for a model where spheres as a tool to maintain self-avoidance are not necessary. This is achieved by a tethered triangulated surface where the triangles are flexible and impenetrable (« flexible impenetrable plaquettes »). This model provides for the first time some evidence that flexible *polymerized* membranes are crumpled. The results from simulations of the plaquette model are reported and discussed below.

2. Model and simulation technique.

Two types of plaquette models have been simulated : « open » membranes with free boundaries and spherically closed membranes called « vesicles ». Vesicles are of interest as models of cell membranes which exhibit many different shapes [2]. Shape transformation can be induced by changing the osmotic pressure [15], the temperature or the composition of lipids.

The initial configuration of a molecular model of a vesicle consists of a spherically closed triangular mesh. Starting from an icosahedron, one adds new points on each triangle followed by a subsequent rescaling of all bonds to the desired length [16]. This procedure insures that most of the grid points have 6 neighbors and each bond has approximately the same length. The vesicles consist of $N = 10 \times 3^k + \chi$ vertices (or « monomers ») with $k \geq 1$. The number of triangles (or « plaquettes ») is $N_p = 2(N - \chi)$ while the number of bonds (or « edges ») is $N_e = 3(N - \chi)$. These quantities satisfy Euler's theorem $N + N_p - N_e = \chi$ where $\chi = 2 - 2g$ is the Euler characteristic, and g is the genus or number of handles of the manifold, which is $g = 0$ for a sphere and $g = 1$ for a torus.

The initial configuration of an *open membrane* with free boundary consists of $N = 3k(k-1) + 1$ vertices ($k \geq 2$) on a triangular mesh, where the shape of the mesh is a hexagon. Accordingly, we have $N_p = 6(k-1)^2$ plaquettes and $N_e = 3(3k-2)(k-1)$ edges or « tethers ».

Each Monte Carlo step consists of randomly selecting a vertex and displacing it to a nearby location which is chosen at random. The variation of the bond length ℓ connecting vertices are restricted to $\ell_{min} < \ell < \ell_{max} = \sqrt{2}$. The minimum length $\ell_{min} = w\ell_{max} (0 < w < 1)$ is the only free parameter of the model. The self-avoidance of the surface is achieved by prohibiting interpenetration of each triangle with any other triangle (« flexible hard plaquettes »). Similar algorithm has been previously applied to entangled « thin » polymer chains [17, 18]. More details about the algorithm will be published elsewhere.

In the present study we report on simulations of vesicles and open membranes with $w = 0.1$ and $w = 0.5$. More extensive simulations of open membranes with $0.1 \leq w \leq 0.7$ are reported elsewhere [19].

Equilibrium averages are taken over up to 10^4 configurations. Correlations between conformations have been analyzed and are discussed in one of the following sections.

3. Results and discussions.

A typical snapshot of a plaquette-vesicle is depicted in figure 1 for 540 plaquettes and bond parameter $w = 0.1$. The various degrees of brigthness of each plaquette is due to mirror reflection techniques. This snapshot demonstrate the highly folded character of the surface.

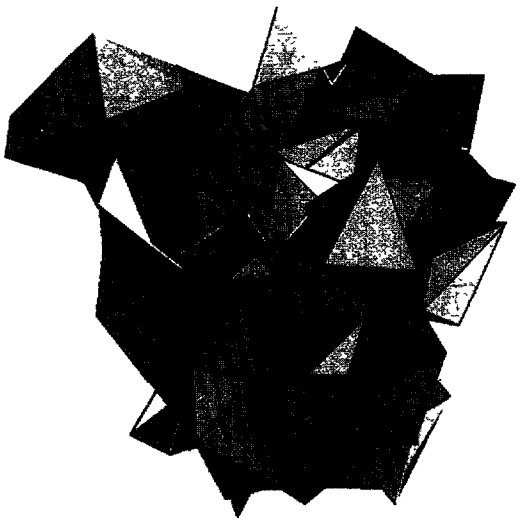

Fig. 1. — Typical snapshot of a crumpled vesicle consisting of 540 plaquettes with bond parameter $w = 0.1$.

The fluctuation of the surface area A

$$\delta A \equiv \sqrt{\langle (A - \langle A \rangle)^2 \rangle} \tag{1}$$

increases according to $\delta A \sim \sqrt{A}$. This indicates that the central limit theorem is valid for δA, i.e., the long-time fluctuations of the extensive quantity A are statistically uncorrelated. The average surface area increases linearly with the number of plaquettes N_p, and the average bond length is independent of N. The corresponding values are listed in table I.

3.1 RADIUS OF GYRATION. — One of the main results from the present Monte Carlo study is the dependency of the mean square radius of gyration R^2 on the average surface area A. This is depicted in figure 2 for two bond parameters $w = 0.1$ and 0.5. All data collapse approximately on a single curve for each of the two models, vesicle and open membrane, almost independently of the bond parameter w, exhibiting $R^2 \sim A^{0.8 \pm 0.01}$ This indicates, that the power law is *independent* of the choice of boundary condition, either spherical as in the case of vesicles or free boundaries as in the case of open membranes, which is analogous to the situation of polymers, where linear chains and polymer rings have the same correlation exponent ν. The fluctuation of the mean square radius of gyration of the vesicles, defined according to equation (1), follows a power law $\delta R^2 \sim A^{0.5 \pm 0.02}$ So far, we have no analytic arguments for $\delta R^2/R^2 \sim A^{-0.3}$ This result is in contrast to hard-sphere models of membranes where $R^2 \sim A$ [6-12].

Table I. — *Mean length of the tethers* $\langle \ell \rangle$, *average area of plaquettes* A/N_p, *normalized fluctuation of the total area* δA *and average angle between plaquettes* U *for two bond parameters* w *and for plaquette models. The first two lines correspond to vesicles, the last two lines to open membranes.*

w	$\langle \ell \rangle$	A/N_p	$(\delta A)^2/A$	U
0.1	0.893	0.285	0.182	0.29
0.5	1.062	0.455	0.065	0.37
0.1	0.908	0.288	0.16	0.280
0.5	1.066	0.456	0.058	0.350

3.2 LOCAL RIGIDITY. — If $\mathbf{n}_\alpha$ denotes the unit normal to the α-th triangular plaquette, the average angle enclosed by two adjacent normals of plaquettes sharing a common edge is

$$U = \frac{1}{N_e} \sum_{\langle \alpha, \beta \rangle} \mathbf{n}_\alpha \, \mathbf{n}_\beta \tag{2}$$

where the sum is over all such pairs $\langle \alpha, \beta \rangle$ of plaquettes on the surface and N_e is the total number of common edges on the surface. The average value of U depends on w. For vesicles, $\langle U \rangle$ is almost independent of N, whereas for open membranes a weak N dependence is observed which is probably due to boundary effects and is expected to vanish for $N \to \infty$. The values of $\langle U \rangle$ for $w = 0.1$ and 0.5 are listed in table I ; the values for open membranes correspond to $N = 271$.

In figure 3, we present a log-log plot of the probability distribution $P(\cos\theta)$ of $\cos\theta \equiv \mathbf{n}_\alpha \cdot \mathbf{n}_\beta$ *versus* $|\cos\theta - 1|$ for bond parameters $w = 0.1$ and 0.5 in the case of the vesicle model. The distribution indicates that plaquette-vesicles are indeed very flexible and the enclosed angles between adjacent plaquettes are not restricted. This is in contrast to pearl-membrane models where due to hard sphere repulsion $P(\cos\theta) \approx 0$ for some $\theta^* > \theta$, where θ^* depends on the hard sphere diameter $\sigma = \ell_{min}/\ell_{max}$. This is demonstrated for $\sigma = 0.6$ and depicted in figure 3. For plaquette-vesicles, the power law $P(\cos\theta) \sim |\cos\theta - 1|^{-0.52}$, as indicated in figure 3, may be qualitatively correct for small angles θ and independent of w, i.e., $P(\cos\theta) \sim \theta^{-1.04}$ for $|\cos\theta - 1| < 1$. The onset of deviation from the power law, as observed in figure 3, may be determined by the bond parameter w.

3.3 CORRELATIONS BETWEEN PLAQUETTES. — In figures 4 and 5, we present the correlation functions $\langle \mathbf{n}(0) \cdot \mathbf{n}(x) \rangle$ between plaquette normals of open membranes and vesicles, respectively, as a function of the scaled distance x/ℓ, where ℓ is the mean length of the tethers. The normal-normal correlation function measures the range of correlation, which is expected to be short ranged for crumpled conformations and long ranged in the rough phase.

According to figure 4 for open plaquette-membranes consisting of $N = 271$ vertices, as an example, the normals are strongly correlated for $x/\ell < 1$. The correlations depend in this range on the bond parameter $w = 0.1$ and $w = 0.6$, but are almost independent of N. For larger distances, the correlations decay rapidly down to $\langle \mathbf{n}(0) \cdot \mathbf{n}(x) \rangle \leq 0.05$. This

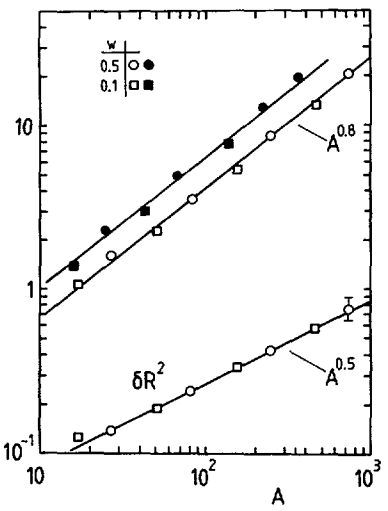

Fig. 2.

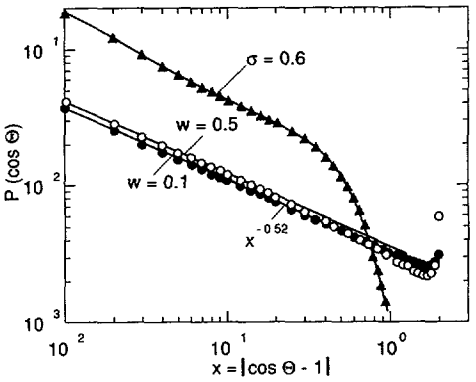

Fig. 3.

Fig. 2. — Log-log plot of the mean square radius of gyration R^2 and the fluctuation δR^2 *vs.* the surface area A for various bond parameters w. The open and the full symbols correspond to plaquette-vesicles and open plaquette-membranes, respectively. The statistical errors are in the order of the size of the symbols.

Fig. 3. — Log-log plot of the probability distribution $P(\cos\theta)$ of the angle θ between adjacent plaquette normals *vs.* $|\cos\theta - 1|$. The lower curves labeled by the bond parameters $w = 0.1$ and 0.5 correspond to plaquette-vesicles, whereas the upper curve labeled by $\sigma = 0.6$ corresponds to pearl-vesicles.

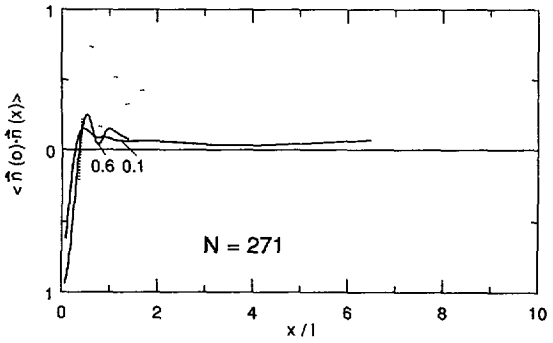

Fig. 4.

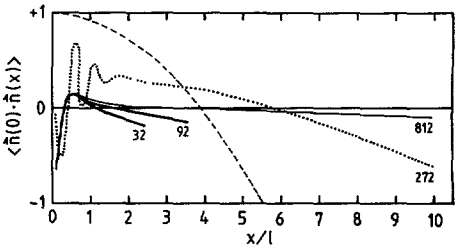

Fig. 5.

Fig. 4. — *Open membrane* : Correlation function between plaquette normals $\langle \mathbf{n}(0)\cdot\mathbf{n}(x)\rangle$ as a function of distance x/ℓ for $w = 0.1$ and $w = 0.6$ for $N = 271$. The dotted curve corresponds to the pearl-membrane model consisting of $N = 271$ spheres of diameter $\sigma = 0.6$.

Fig. 5. — *Vesicle* : Correlation function between plaquette normals $\langle \mathbf{n}(0)\cdot\mathbf{n}(x)\rangle$ as a function of distance x/ℓ for $w = 0.1$ and various N. The dotted curve corresponds to the pearl-vesicle model consisting of $N = 272$ spheres of diameter $\sigma = 0.6$.

behaviour is in contrast to that of the pearl-membrane model whose correlations are depicted by the dotted curve in figure 4. In order to compare the hard-sphere model with the plaquette model of $w = 0.5$, we have chosen a hard-sphere diameter of $\sigma = 0.6$. For $x/\ell < 1$, the pearl-membrane model exhibits much stronger correlations as compared to the plaquette model. At distances $x/\ell > 1$, the correlations remain finite, $\langle \mathbf{n}(0) \cdot \mathbf{n}(x) \rangle \approx 0.3$, which is in contrast to the plaquette model. The small upward bending of the correlation function for large x/ℓ, as observed in figure 4, is related to the finite extensibility of the network leading to flat conformations at large extensions. It should be noted that the behaviour of the normal-normal correlation function as depicted for $N = 271$ in figure 4 is qualitatively the same for smaller as well as for larger N ($N = 91$, 169, 397, 721 [19]), and the short range behaviour and the plateau value are almost independent of N.

Similar conclusions concerning $\langle \mathbf{n}(0) \cdot \mathbf{n}(x) \rangle$ are provided by the results from plaquette-vesicles in comparison to pearl-vesicles, which is depicted in figure 5. The behaviour of $\langle \mathbf{n}(0) \cdot \mathbf{n}(x) \rangle$ for short distances $x/\ell < 1$ is similar as in the case of open membranes. For larger distances the correlation functions become negative. This is a reminiscence of the spherical character of the vesicle surface. For comparison the broken line in figure 5 corresponds to an inflated vesicle of size $N = 92$, demonstrating the effect of the spherical boundary condition. One observes that the crossover to negative values occurs at the size of the radius of gyration R of the vesicles which are for the plaquette-vesicles, $R = 1.05$, 2.0, 3.6 for $N = 32$, 92, 812, respectively. But the main observation is, similar as in the case of open membranes, that the correlations in the pearl-vesicle (with $\sigma = 0.6$, represented by the dotted line in Fig. 5) are much larger than in the comparable plaquette-vesicle with $w = 0.5$.

In summary, the correlations between the normals in the plaquette model are qualitative different from the correlations in the hard-sphere model. The correlation function of the pearl-membrane model varies strongly at shorter distances and looks similar to the pair correlation function of classical hard sphere fluids. At larger distances the normals of the plaquette model are almost uncorrelated, whereas the correlations of the hard-sphere model remain finite. It is conceivable that the observed strong correlation effects in the hard-sphere model are responsible for the absence of crumpled conformations.

3.4 DYNAMICS. — In the following section we discuss some dynamical properties of plaquette-vesicles. We restrict our attention to the time dependent correlation function of the mean square radius of gyration

$$\Phi_R(t) = \frac{\langle R^2(0)\, R^2(t) \rangle - \langle R^2 \rangle^2}{\langle R^4 \rangle - \langle R^2 \rangle^2} \tag{3}$$

The amount of decay of $\Phi_R(t)$ provides some information how far our estimates of various static quantities as discussed above are based on uncorrelated data. The correlation function $\Phi_R(t)$ is depicted in figure 6. For comparison, it should be noted that the total Monte Carlo time τ_{MC} the vesicles were simulated (one MC time step is one attempted move per vertex), was $\tau_{MC} \approx 3\,600$ for $N = 272$ and $\tau_{MC} \approx 400$ for $N = 812$. This has to compared with the time during which $\Phi_R(t)$ decayed to $1/e$. Since $\Phi_R(t) < 0.2$ for $t \ll \tau_{MC}$ as shown in figure 6, τ_{MC} can be considered to be sufficiently long in order to obtain well equilibrated data.

In figure 6 we have depicted $\Phi_R(t)$ *versus* t/N in a semi-log plot. Since $\Phi(t/N)$ is almost independent of N and an exponential relaxation is observed for $\Phi_R(t) > 0.2$ for both $w = 0.1$ and 0.5, the typical correlation is in the order of $\tau \sim N$.

On the other hand, this result is somewhat unexpected, because classical Rouse behavior $\tau \sim N^{1+\nu}$ ($\nu \approx 0.8$), analogous to free-draining single polymers, should appear and has been

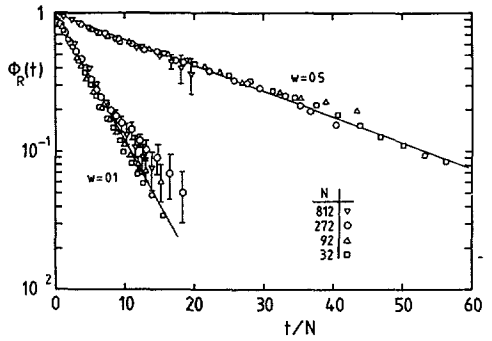

Fig. 6. — Semi-log plot of the time correlation function of the mean square radius of gyration $\Phi_R(t)$ *vs.* the scaled time t/N for bond parameters $w = 0.1$ and 0.5 for the plaquette-vesicle model.

predicted and discussed in detail for open polymerized membranes [5]. The disagreement could be resolved by relating this phenomena to a crossover effect which requires separate considerations of « gel-like » longitudinal modes and Rouse relaxation. For « in-plane » longitudinal relaxation we expect $\tau_1 \sim N$, similar as in permanent cross-linked networks [20, 21] and « phantom » membranes [5], whereas for out-of-plane relaxation $\tau_2 \sim N^{1+\nu}$ Assuming that $\Phi_R(t)$ can be represented by the sum of two exponentials

$$\Phi_R(t) = a_1 \exp(-t/\tau_1) + a_2 \exp(-t/\tau_2)\,, \tag{4}$$

then the typical time τ^* characterizing the crossover between gel-like relaxation and Rouse relaxation is $\tau^* \approx \tau_1 \ln(a_1/a_2)$. If $a_1/a_2 \gg 1$, then the two relaxation processes could be well separated. Assuming $a_1 \approx 1$, then the time τ_1 can be estimated according to the time during which $\Phi_R(t)$ decayed to $1/e$ from its initial value. In this case we obtain estimates $\tau_1 = 4.2\,N$ and $22\,N$ for $w = 0.1$ and 0.5, respectively. Since for $t > \tau^*$ the correlation function is $\Phi_R(t) < 0.1$ and is rather noisy due to large statistical fluctuations (compare Fig. 6), the possible appearance of Rouse relaxation is difficult to confirm and cannot be excluded. It is unknown how the ratio a_1/a_2 depend on the bond parameter w.

4. Concluding remarks.

In summary, the present Monte Carlo study of a new model for polymeric self-avoiding surfaces indicates that the conformations of polymerized membranes with sufficiently small intrinsic rigidity are crumpled with a fractal dimension of $D = 2.5$. This supports analytical predictions [5] and recent experimental evidence [14]. It supports the conjecture [12] that hard-sphere models of polymerized surfaces [5-12] have strong internal correlations preventing the membrane from crumpling.

It should be noted that similar crumpling phenomena and the same fractal dimension have been found recently for « fluid » self-avoiding surfaces too [10, 11]. Polymerized and fluid models differ with respect to the local coordination number q_i of the vertices i of the triangulated surface. In contrast to polymerized surfaces, the numbers q_i are not conserved in the fluid model, although in both cases $\sum_{i=1}^{N} q_i = 3(N-2)$. This leads to the interesting question whether the coincidence of the fractal dimensions of fluid and polymerized surfaces is exact, and wether membrane models with quenched connectivity belong to the same class as fluid models with a locally fluctuating metric.

Finally it should be mentioned that the fractal dimension of 2.5 for self-avoiding polymerized surfaces, as reported in the present work, has been found recently also for surfaces (or « hulls ») of percolation clusters [22]. This raises the intriguing question wether the two models are related to each other and belong to the same universality class.

Acknowledgements.

I am very grateful to R. Lipowsky and W. Renz for interest and useful comments. The simulations were performed on the CRAY X-MP/416 at the Forschungszentrum Jülich.

References

[1] Statistical Mechanics of Membranes and Surfaces, D. R. Nelson, T. Piran and S. Weinberg Eds. (World Scientific, 1989).
[2] LIPOWSKY R., *Nature* **349** (1991) 475.
[3] NELSON D. R. and PELITI L., *J. Phys. France* **48** (1987) 1085.
[4] KANTOR Y. and NELSON D. R., *Phys. Rev. A* **36** (1987) 4020.
[5] KANTOR Y., KARDAR M. and NELSON D. R., *Phys. Rev. A* **35** (1987) 3056.
[6] PLISCHKE M. and BOAL D., *Phys. Rev. A* **38** (1988) 4943.
[7] ABRAHAM F. F., RUDGE W. and PLISCHKE M., *Phys. Rev. Lett.* **62** (1989) 1757.
[8] HO J.-S. and BAUMGÄRTNER A., *Phys. Rev. Lett.* **63** (1989) 1234.
[9] BOAL D., LEVINSON E., LIU D. and PLISCHKE M., *Phys. Rev. A* **40** (1989) 3292.
[10] BAUMGÄRTNER A. and HO J.-S., *Phys. Rev. A* **41** (1990) 5747.
[11] HO J.-S. and BAUMGÄRTNER A., *Europhys. Lett.* **12** (1990) 295.
[12] ABRAHAM F. F., NELSON D. R., *J. Phys. France* **51** (1990) 2653.
[13] MUTHUKUMAR M., *J. Chem. Phys.* **88** (1988) 2854.
[14] HWA T., KOKUFUTA E., TANAKA T., *Phys. Rev. A* (1991).
[15] KOMURA S., BAUMGÄRTNER A., *Phys. Rev. A* (1991).
[16] HO J.-S. and BAUMGÄRTNER A., *Mol. Simul.* **6** (1991) 163.
[17] BAUMGÄRTNER A., *Polymer* **22** (1981) 1308.
[18] BAUMGÄRTNER A., BINDER K., *J. Chem. Phys.* **75** (1981) 2994.
[19] BAUMGÄRTNER A., RENZ W. (to be published).
[20] DE GENNES P. G., *Macromolecules* **9** (1976) 587.
[21] TANAKA T., HOCKER L., BENEDEK G. B., *J. Chem. Phys.* **59** (1973) 5151.
[22] STRENSKI P. N., BRADLEY R. M., DEBIERRE J. M., *Phys. Rev. Lett.* **66** (1991) 1330.